



Murdoch
UNIVERSITY

MURDOCH RESEARCH REPOSITORY

This is the author's final version of the work, as accepted for publication following peer review but without the publisher's layout or pagination.

The definitive version is available at

<http://dx.doi.org/10.1016/j.mssp.2012.07.006>

**Al-Taay, H.F., Mahdi, M.A., Parlevliet, D. and Jennings, P. (2013)
Controlling the diameter of silicon nanowires grown using a tin
catalyst. Materials Science in Semiconductor Processing,
16 (1). pp. 15-22.**

<http://researchrepository.murdoch.edu.au/12377/>

Copyright: © 2012 Elsevier Ltd

It is posted here for your personal use. No further distribution is permitted.

Controlling the diameter of silicon nanowires grown using a tin catalyst

H.F. Al-Taay^{a, b}, M.A. Mahdi^c, D. Parlevliet^a, P. Jennings^a

^a School of Engineering & Energy, Murdoch University, South Street, Murdoch, WA 6150, Australia

^b Department of Physics, College of Sciences for Women, University of Baghdad, Baghdad, Iraq

^c Nano-Optoelectronics Research and Technology Laboratory (N.O.R.), School of Physics, Universiti Sains Malaysia, 11800 Penang, Malaysia

Abstract

Silicon nanowires were grown on ITO-coated glass substrates via a pulsed plasma enhanced chemical vapor deposition method, using tin as a catalyst. The thin films of catalyst, with different thicknesses in the range 10–100 nm, were deposited on the substrates by a thermal evaporation method. The effect of the thickness of the thin film catalyst on the morphology of the silicon nanowires was investigated. The scanning/transmission electron microscopy images showed that the wire diameter increased as the thickness of the thin film catalyst increased. The nanowires grown using a thin film thickness of 10 nm were inhomogeneous in diameter, whereas the other thicknesses led to an increase in the homogeneity of the diameters of the nanowires. The dominant wire diameter of the grown silicon nanowires ranged from 70 to 80 nm with 10 nm catalyst thin film thickness, and increased to a range of 190–200 nm with 100 nm catalyst thin film thickness.

Keywords: Silicon nanowires; Tin catalyst; Wire diameter control

Introduction

In the past decade, one-dimensional (1D) nanostructured semiconductors, such as nanowires, nanorods, nanotubes, nanoribbons and nanosheets have attracted extraordinary attention because of their unique physical and chemical properties. For example, 1D semiconductors have several unique advantages, including high crystallinity, self-assembly, high surface-to-volume ratio, quantum confinement effects as well as slow electron–hole recombination that allow them to be used in novel miniaturized electronic, optoelectronic as well as energy conversion and storage devices [1], [2], [3], [4], [5], [6], [7] and [8]. The physical properties of nanostructured materials are dependent on their shape and dimensions; therefore, controlling these two parameters has become an urgent necessity. For 1D nanostructured materials, there is a need to control the diameter to fabricate high-quality devices.

One of the most important 1D nanostructured materials is the silicon nanowire (SiNW), which has unique physical properties, making it a popular material for a variety applications [9] and [10].

Chemical Vapor Deposition (CVD) is one of the most common methods used to grow SiNWs [11]. The nanowires which are prepared by the CVD method are grown via the Vapor–Liquid–Solid (VLS) mechanism that requires metal catalysts. The gold (Au) seed particle is the material most commonly used as a catalyst for the synthesis of SiNWs due to its high chemical stability, its lack of toxicity and its eutectic point at about 19% Si is relatively low [12]. Thus, there are many applications based on SiNWs grown using a Au catalyst, such as solar cells [13] and [14] and energy storage devices [8]. However, the disadvantage of using Au as a catalyst is that it has energy levels close to the Si band-gap middle. Thus it acts as a deep-level defect in the band gap of Si and contributes to the reduction of the minority charge-carrier lifetime by providing centers for charge-carrier recombination [15] and [12]. Another reason that must be taken into consideration is that gold is an expensive metal.

Titanium (Ti) and platinum (Pt) have also been used to catalyze SiNWs. However, Ti and Pt can form intermediate compounds, such as silicides; moreover, they need high temperatures of 1330 and 979 °C for Ti–Si and Pt–Si eutectics, respectively. A high synthesis temperature is required for VLS growth of Si wires using Ti and Pt as catalysts [16] and [17]. Tin (Sn) is a promising metal catalyst candidate for low-temperature synthesis because the Sn–Si alloy has a low eutectic temperature of 232 °C. The low eutectic temperature provides new opportunities to lower the growth temperature of SiNWs produced via the VLS mechanism, which would also be favorable for device integration [18] and [19].

There are several different methods that can be used to grow SiNWs, and these affect the morphology, density, and presence of defects in the wires. Various methods have been used to synthesize SiNWs, such as laser ablation (LA), thermal evaporation (TE), chemical vapor deposition (CVD), and plasma enhanced chemical vapor deposition (PECVD) [20], [21], [22] and [23].

In the present study, the Pulsed Plasma Enhanced Chemical Vapor Deposition (PPECVD) method has been used to grow SiNWs on ITO-coated glass substrates using Sn as a catalyst. Controlling the morphology and diameter of SiNWs by controlling the thickness of the catalyst thin film have also been investigated. Further, the effect of the thickness of the catalysts used in controlling the diameter of the SiNWs has been determined.

Experimental details

Thin films of the Sn catalyst, with varying thicknesses in the range of 10–100 nm, were prepared by the thermal evaporation method on ITO-coated glass substrates at room temperature. ITO-coated glass substrates are widely used for optoelectronic device fabrication, and this is the focus of our work. The thickness of the Sn thin films was controlled by a quartz crystal microbalance installed in the thermal evaporation chamber.

The samples were loaded into the PECVD chamber, argon was introduced with a pressure of 3 Torr and the temperature was increased gradually to 400 °C over 35 min. Then, pure silane gas (SiH_4) was admitted to the system as a Si source. A square wave generated by a pulse generator (SRS model DGS 35) was used to modulate the 13.56 MHz, 30 W power signal used to generate the plasma, using a modulation frequency of 1000 Hz. The total preparation time was 40 min. After the growth process was completed, the system was purged with argon and cooled to room temperature.

The nanowire morphology was examined using a Scanning Electron Microscope (SEM) (Phillips XL 20 SEM) and Transmission Electron Microscopy (TEM) (Philips CM 100 TEM). X-ray diffraction (XRD; PANalytical X'Pert PRO with $\text{Cu K}\alpha$ ($\lambda=1.5406 \text{ \AA}$) radiation) was employed to determine the crystalline structure of the prepared SiNWs.

Results and discussion

Morphology

Fig. 1 shows the SEM images of the SiNWs nanowires grown on the ITO-coated glass substrates with Sn thin film catalysts having different thicknesses. The SEM images showed that the SiNWs were

tapered. For the SiNWs grown using the 10 nm thin film Sn catalyst, the SiNWs appear to be inhomogeneous in diameter and the wires are tapered at the end (Fig. 1A). Using a Sn catalyst thin film with 20 nm thickness, resulted in the prepared SiNWs having a more homogenous diameter. The tapered end occurred in some wires (Fig. 1B) and completely disappeared when the film thickness of 40 nm was used (Fig. 1C). The droplet sizes with 10 and 20 nm catalyst thin films are relatively small compared with the other thicknesses used, thus the small droplets apparently did not control the growth of the wires, due to the loss of Sn into the SiNWs. The SiNWs grown using 60, 80, and 100 nm film thicknesses showed significant improvements in the morphology of the wires, especially in terms of the diameter homogeneity (Fig. 1D–F).

To identify the optimal Sn thin film thickness for growing SiNWs, the diameter distribution was calculated, as shown in Fig. 2. The wire diameter increased with the increase in the thickness of the catalyst thin films (Fig. 2). The diameters of the SiNWs ranged from 60 to 110 nm with a catalyst thickness of 10 nm and increased to a range of 80–130 nm with use of 20 nm Sn thin film catalysts. Furthermore, the range of diameters of the SiNWs for the samples prepared using a Sn thin film thickness of 100 nm was 160–220 nm.

Fig. 3 shows the linear relationship between the Sn thin film thickness and the modes of the SiNW diameter distributions. The mode of the average diameters was found to increase linearly as the Sn catalyst film thickness increased. Fig. 3 also shows the relationship between the thickness of the catalyst thin films and the resulting average catalyst droplet diameter calculated from the SEM images of each sample. It was observed that an increase in the thickness of the Sn thin films led to an increase in droplet diameter, which in turn led to the increase in the diameter of the grown SiNWs. This allows the average diameter of the nanowires to be selected by using the appropriate catalyst layer thickness. The cross-sectional FESEM images of SiNWs prepared using 20, 60 and 100 nm Sn thin film

thicknesses are shown in Fig. 4. The average lengths of SiNWs catalyzed by 20 and 100 nm Sn thin films were 4.1 and 3.7 μm , respectively.

Fig. 5 shows the TEM images of SiNWs prepared using Sn catalyst thin film thicknesses of 20, 60 and 100 nm, respectively. The TEM images confirmed that the grown wire diameters increased as the catalyst film thickness increased. As shown in Fig. 5, the diameter of SiNWs prepared using 20 and 60 nm Sn thin film thicknesses ranged from 95 to 105 nm while it ranged from 170 to 195 nm for the SiNWs catalyzed by 100 nm Sn thickness. The Sn droplets did not show up clearly on the wire tip except for one wire in the 20 nm Sn catalyst sample, showing that the growth mechanism producing SiNWs was the VLS mechanism. The surface tension value of Sn liquid is 0.6 J m^{-2} [12], which is lower than the required value (0.85 J m^{-2}) to make the droplets sit on the wire end [12] thus, the Sn droplets easily fell off when the TEM samples were prepared using ultrasonics.

The Sn–Si phase diagram (Fig. 6) [9] shows that the Sn melting point is about $232 \text{ }^\circ\text{C}$. During the growth process, at a temperature of $400 \text{ }^\circ\text{C}$, and before the SiH_4 gas is introduced into the PECVD chamber, the Sn particles melted and aggregated to form large droplets due to surface tension.

Furthermore, when the Sn droplets were exposed to SiH_4 gas, the gas molecules disintegrated at the surface of the Sn droplets in the Si dissolved in the Sn and formed the Sn–Si liquid phase. The eutectic point of Sn–Si is very low at about $232 \text{ }^\circ\text{C}$ with a silicon ratio less than 1% compared with other catalyst metals, such as Au ($363 \text{ }^\circ\text{C}$, Si of 19%) and Al ($577 \text{ }^\circ\text{C}$, Si of 12%) [12]. Thus, the Sn–Si liquid phase formed at very low Si concentration, and thus a low pressure of Si atoms was required when using Sn to grow SiNWs, which is potentially very cost effective.

A few preliminary studies have been reported for Sn-catalyzed SiNWs. A hydrogen radical-assisted deposition method has been used to synthesize SiNWs for the studies of the effects of metal catalyst

thickness. It has been shown previously for other growth techniques, yet not for the PPECVD method, that the nanowire diameter is determined by the size of the catalyst droplet which nucleates the nanowire. The findings show that SiNWs produced using a relatively thin layer (30 nm thick) of Sn catalyst are better arranged and controlled than those produced on relatively thick Sn-coated catalysts (100 nm thick) [24]. Jeon and Kamisako used a 7 nm thick Sn catalyst at 400 °C to grow SiNWs by VLS and also obtained a homogenous diameter [25].

Cui et al. [26] found that the diameter of the catalyst droplet determines the size of the nanowire because the diameter of SiNWs increases with the thickness of Au nanoclusters. The authors also found that the Au–Si alloy droplet diameter is consistently smaller than the diameter of the nanowire during the formation.

Our results are also in accordance with those presented by Wacaser et al. [27], which show the effect of varying the thickness of the Al layer. They also showed that the average diameter of the nanowire increases with the thickness of the Al layer.

In most cases of catalyzed growth of NWs prepared by the VLS mechanism, the diameter of the catalyst droplet (D_c) exceeds the diameter of the nanowire (D_w). The relationship between the radius of the catalyst droplet (R) and the wire radius (r) depends on two parameters, the surface tension of the liquid catalyst (σ_L) and the tension of the liquid/solid interface (σ_{LS}) as shown in the equation below [12]

$$R = r \sqrt{\frac{1}{1 - \left(\frac{\sigma_{LS}}{\sigma_L}\right)^2}}, \quad (1)$$

where $R = D_c/2$ and $r = D_w/2$.

Eq. (1) can be rewritten as

$$\left(\frac{r}{R}\right)^2 = 1 - \left(\frac{\sigma_{LS}}{\sigma_L}\right)^2 \quad (2)$$

From Eq. (2), the wire radius approaches the value of the catalyst radius when the σ_L value is much larger than σ_{LS} . The radius of the Sn catalyst droplets used to produce the silicon nanowires in this work are calculated from SEM images and listed in Table 1. The σ_L value of Sn is 0.6 [12], which is more than the σ_L values of Bi, Sb and Pb, but less than those of Ag, Au, and Al [12] and [28]. The liquid/solid interface tension of the grown SiNWs is calculated from Eq. (2). The SiNWs prepared with 10 nm catalyst thin film thickness have the biggest σ_{LS} of 0.37 while the wires grown using a 60 nm thickness had the lowest σ_{LS} value of 0.11 because the radii of the wires and catalyst are very close (Table 1). The contact angle β is expressed by the following equation [12]:

$$\sigma_L \cos(\beta) = -\sigma_{LS} \quad (3)$$

Comparing Eqs. (3) and (2), the contact angle between the catalyst metal and the wire surface can be calculated using Eq. 4

$$\left(\frac{r}{R}\right)^2 = 1 - [-\cos(\beta)]^2 = 1 - \cos^2(\beta) \quad (4)$$

The minimum β value was 101° for SiNWs catalyzed by 60 nm thick Sn thin films and the maximum value was 129° for the wires prepared with 10 nm thin film thickness.

Fig. 7 shows the surface tension of the liquid catalyst and the direction of the surface tension at the liquid/solid interface, in addition to the contact angle.

At a high substrate temperature, the molten droplets increase in diameter, which leads to the readjustment of the chemical composition of the droplets so that they can cope with the material change at the liquid–solid interface. This process leads to the surface curving out and taking a spherical shape. The droplets take an ellipsoidal shape, with a radius that is larger than that of the wire, depending on the degree of its stability and surface energy [29]. Moreover, there is some change in the contact angle due to the difference in shape between the droplets on the substrate surface and those on the top of the Si wire. Thus, this transition in droplet shape during the growth process will lead to some expansion of the wire base. However, there is no observed change in the prepared SiNW's diameter along the wire length, which could mean no effective change in droplet shape during the growth process.

The average wire density per unit area was calculated from SEM images and found to decrease from 17 to 8 wires/ $(\mu\text{m})^2$ as the thickness of the catalyst thin films increased from 10 to 100 nm (see Table 1).

X-ray diffraction

Fig. 8 shows the XRD patterns of SiNWs prepared using different Sn catalyst thin film thicknesses. All of the XRD patterns show a diffraction peak at an angle of 30.66° corresponding to the ITO-coated glass substrate (Fig. 8 B). The absence of Si diffraction peaks indicated that the samples did not have a crystalline structure. Parlevliet and Jennings have shown previously that SiNWs synthesized by PPECVD with a Sn catalyst are entirely amorphous [23]. Moreover, SiNWs grown by PECVD using Al as a catalyst on Si at 600°C were also amorphous in structure [30]. Yu et al. studied the growth temperature effect on the structure and properties of the SiNWs produced by Sn-catalyzed PECVD [31].

Conclusions

SiNWs were successfully synthesized on ITO/glass substrates using the PPECVD method with Sn droplets as catalysts. The SEM images showed that an increase in the thickness of the Sn catalyst thin films resulted in the increased diameter of the SiNWs. The catalyst film thickness provided good control over the wire diameter, except for a thickness of 10 nm. The catalyst thin film thickness of 60 nm yielded a close match of the catalyst droplet size to the wire diameter with a value of 1.02. Other parameters, such as metal/wire contact angle and tension of the liquid/solid interface, had lower values when the catalyst thin film thickness of 60 nm was used. Thus, the thin film Sn catalyst thickness of 60 nm was judged to be optimal for controlling the growth of the wire diameter. Furthermore, the density of the SiNWs on the ITO surface decreased from 18 to 8 wires/ $(\mu\text{m})^2$ as the Sn catalyst thin film thickness increased from 10 to 100 nm.

Acknowledgment

The authors gratefully acknowledge support from the School of Engineering and Energy, Murdoch University.

References

1. G. Rosaz, B. Salem, N. Pauc, P. Gentile, A. Potié, T. Baron, *Microelectronic Engineering*, 88 (2011), pp. 3312–3315
2. Y. Cui, Z. Zhong, D. Wang, W. Wang, C. Lieber, *Nano Letters* 3 (2003) 149–152.
3. Z. Zhong, D. Wang, Y. Cui, M.W. Bockrath, C.M Lieber, *Science* 302 (2003) 1377–1379.
4. M.A. Mahdi, J.J. Hassan, S.S. Ng, Z. Hassan, Naser M. Ahmed, *Physica E* 44 (2012) 1716–1721.
5. T. Zhai, L. Li, X. Wang, X. Fang, Y. Bando, D. Golberg, *Advanced Functional Materials* 20 (2010) 4233–4248.
6. K. Yu, J. Chen, *Nanoscale Research Letters* 4 (2009) 1–10.
7. B. Tian, X. Zheng, T. Kempa, Y. Fang, N. Yu, G. Yu, J. Huang, C. Lieber, *Nature* 449 (2007) 885–889.

8. C.K. Chan, H. Peng, G. Liu, K. McIlwrath, X.F. Zhang, R.A. Huggins, Y. Cui, *Nature* 3 (2008) 31–35.
9. B. Bhushan, *Springer Handbook of Nanotechnology*, Springer Science + Business Media, Inc, New York, USA, 2007.
10. C. Yoon, K. Cho, J.H. Lee, D. Whang, B.M. Moon, S. Kim, *Solid State Sciences* 12 (2010) 745–749.
11. R.S. Wagner, W.C. Ellis, *Journal of Applied Physics* 35 (1964) 2993–3000.
12. V. Schmidt, J.V. Wittemann, S. Senz, U. Gosele, *Advanced Materials* 21 (2009) 2681–2702.
13. N.J. Quidron, T.I. Kamins, *Nano Letters* 8 (2008) 4410–4414.
14. J. Goldberger, A. Hochbaum, R. Fan, P. Yang, *Nano Letters* 6 (2006) 973–977.
15. D.A. Fraser, *The Physics of Semiconductor Devices*, Clarendon press, Oxford University Press, New York, USA, 1986.
16. S. Sharma, T.I. Kamins, R. Stanley, *Journal of Crystal Growth* 267 (2004) 613–618.
17. R.S. Wagner, W.C. Ellis, *Transactions of the Metallurgical Society of AIME* 233 (1965) 1053–1054.
18. R.W. Olesinski, G.J. Abbaschian, *Bull Alloy Phase Diagram* 5 (1984) 273–275.
19. L. Yu, B. Odonnell, P. Alet, *Nanotechnology* 20 (2009) 225604–225609.
20. N. Fukata, T. Oshima, K. Murakami, T. Kizuka, T. Tsurui, S. Ito, *Applied Physics Letters* A 86 (2005) 213112–213115.
21. H. Pam, S. Lim, C. Poh, H. Sun, X. Wu, Y. Feng, J. Lin, *Nanotechnology* 16 (2005) 417–421.
22. Y. Ke, X. Weng, J.M. Redwing, C.M. Eichfeld, T.R. Swisher, S.E. Mohny, Y.M. Habib, *Nano Letters* 9 (2009) 4494–4499.
23. D. Parlevliet, P. Jennings, *Journal of Nanoparticle Research* 13 (2011) 4431–4436.
24. M. Jeon, K. Kamisako, *Current Applied Physics* 10 (2010) 5191–5195.
25. M. Jeon, K. Kamisako, *Materials Letters* 63 (2009) 777–779.
26. Y. Cui, L.J. Lauhon, M.S. Gudiksen, J. Wang, C.M. Lieber, *Applied Physics Letters* 78 (2001) 2214–2216.
27. B.A. Wacaser, M.C. Reuter, M.M. Khayyat, F.M. Ross, *Nano Letters* 9 (2009) 3296–3301.
28. J. Goloechen, C. Garcia, *Journal of Materials Science* 27 (1992) 5247–5252.
29. S.N. Mohammad, *Journal of Applied Physics* 106 (2009) 104311–104322.
30. F. Iacopi, P.M. Vereecken, M. Schaekers, H. Griffiths, *Nanotechnology* 18 (2007) 505307–505314.
31. L. Yu, P. Alet, G. Picardi, P. Rocai, *Nanotechnology* 19 (2008) 485605–485610.

Fig. 1. SEM images for SiNWs prepared using Sn catalyst thickness of: (A) 10 nm, (B) 20 nm, (C) 40 nm, (D) 60 nm, (E) 80 nm, and (F) 100 nm.

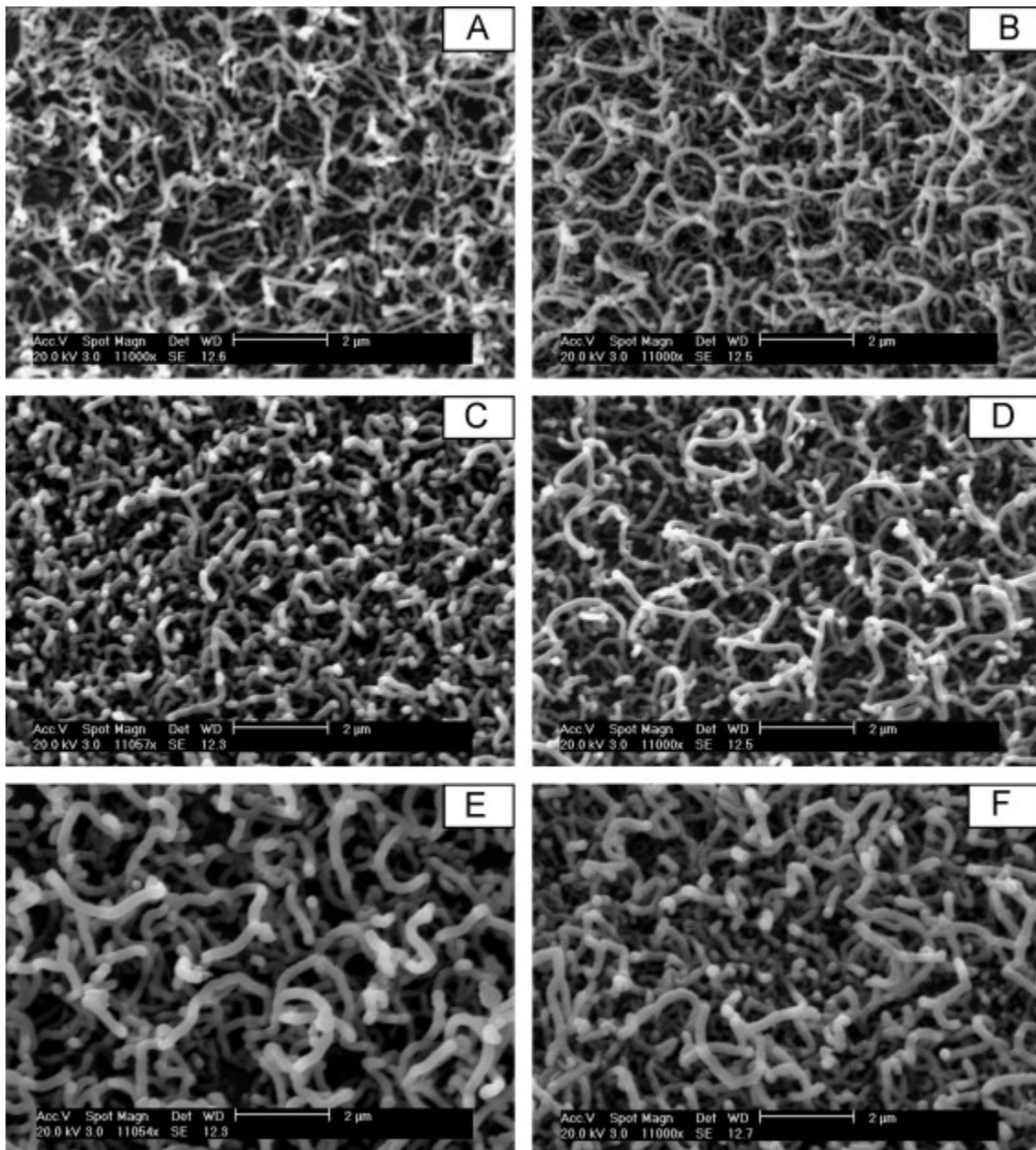


Fig. 2. Diameter distribution of grown SiNWs.

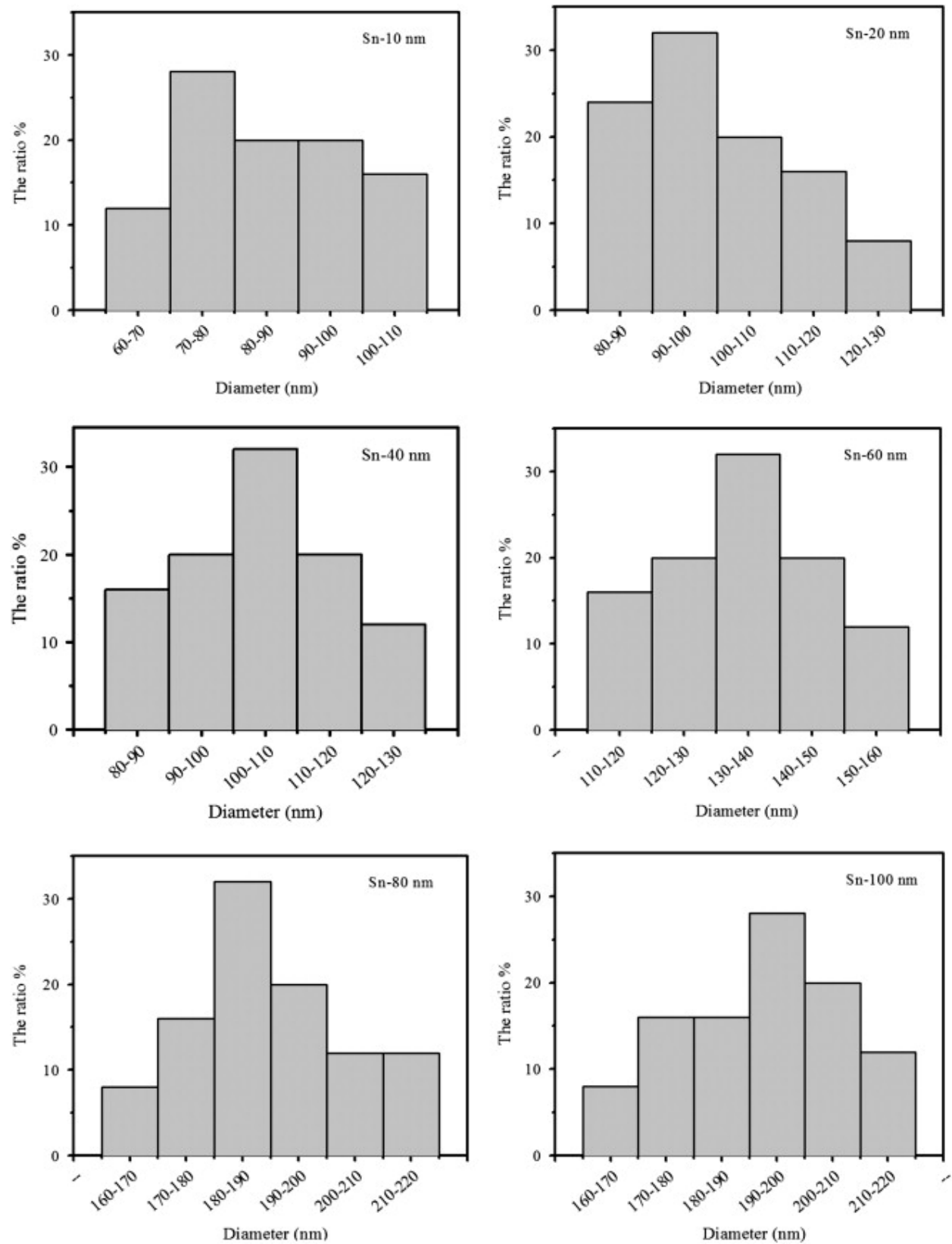


Fig. 3. The catalyst and modal diameter of grown SiNWs vs. Sn thin film thickness.

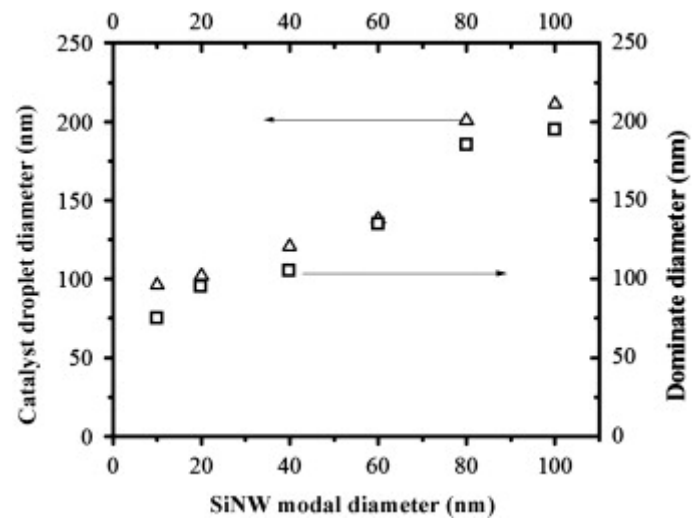


Fig. 4. Cross-sectional images for SiNWs synthesized using Sn catalyst thickness of: (A) 20 nm, (B) 60 nm, and (C) 100 nm.

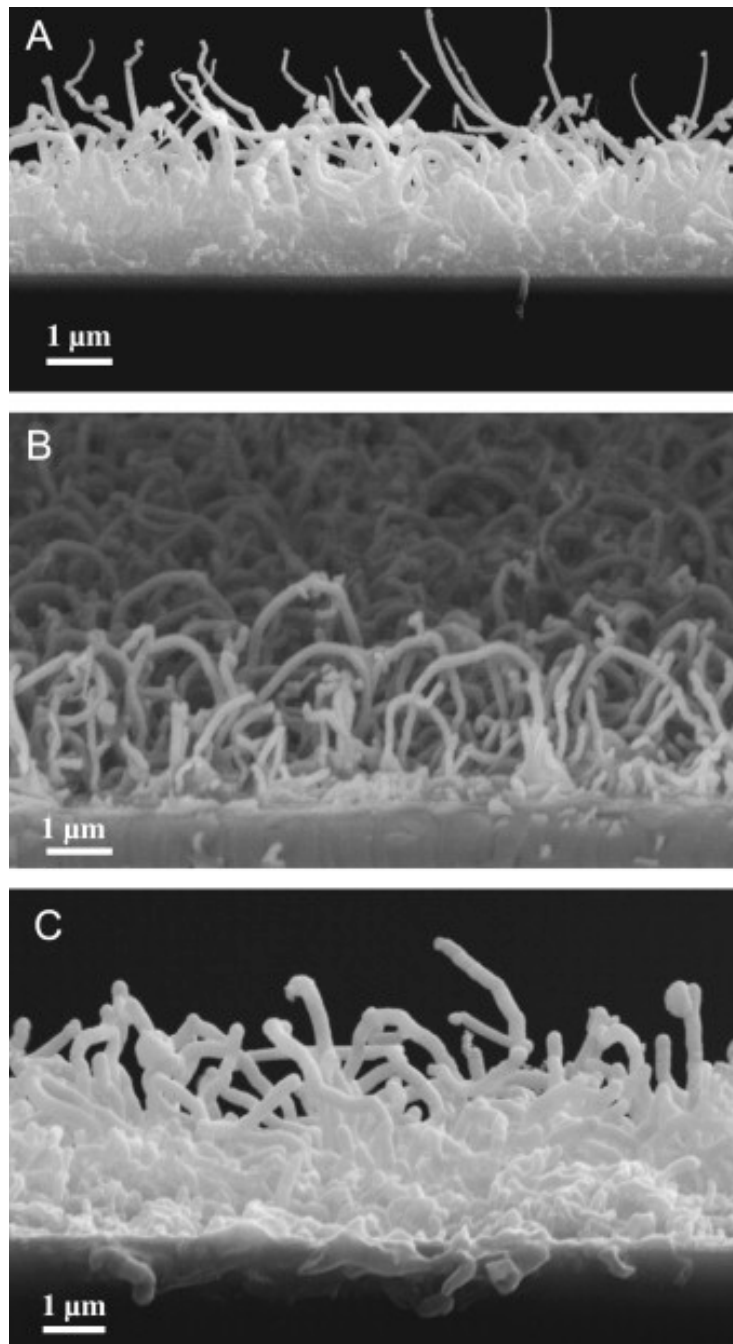


Fig. 5. TEM images of SiNWs prepared by Sn catalyst thin film thickness of: (A) 20 nm, (B) 60 nm, and (C) 100 nm.

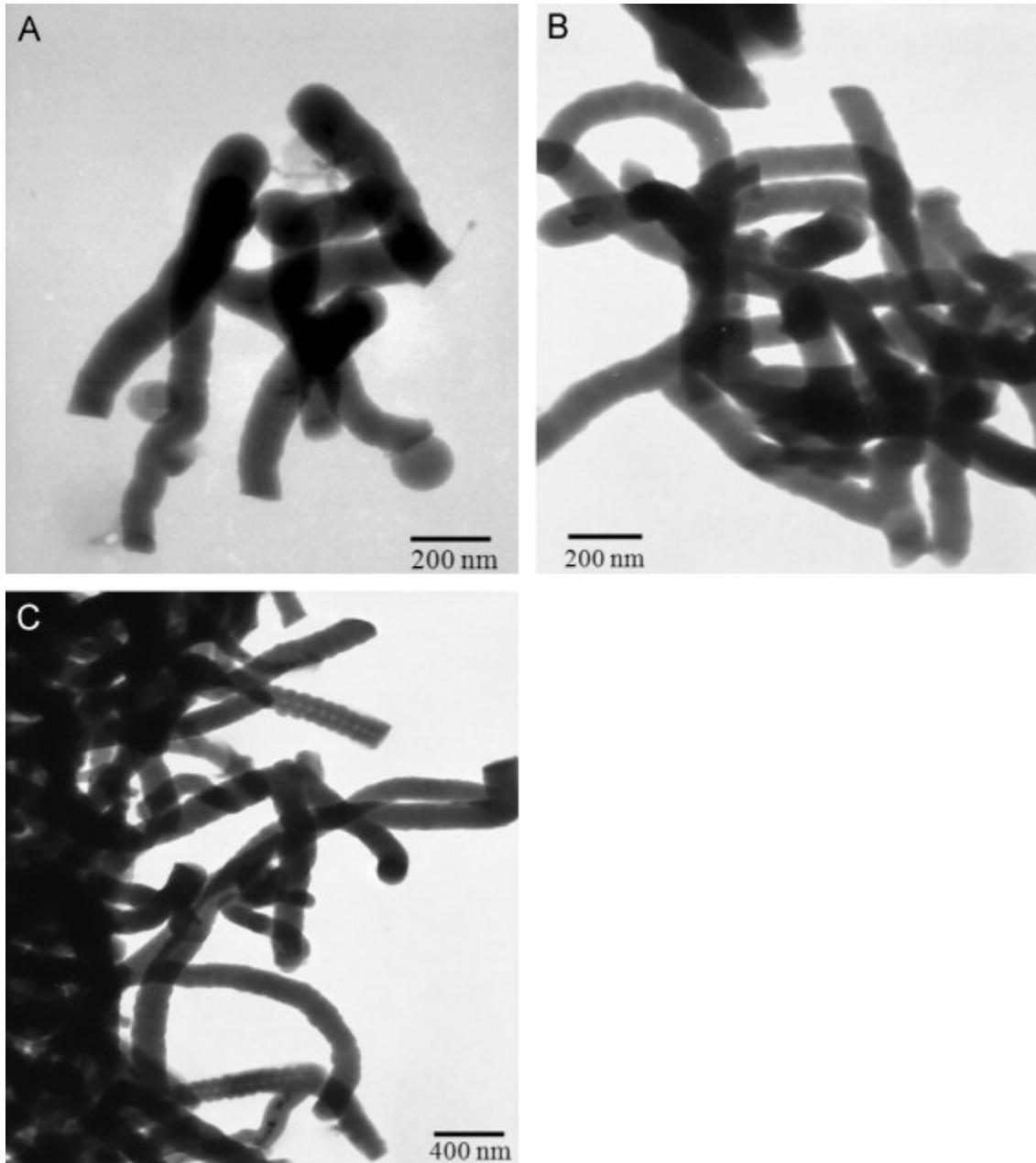


Fig. 6. The Sn–Si alloy binary phase diagram [17].

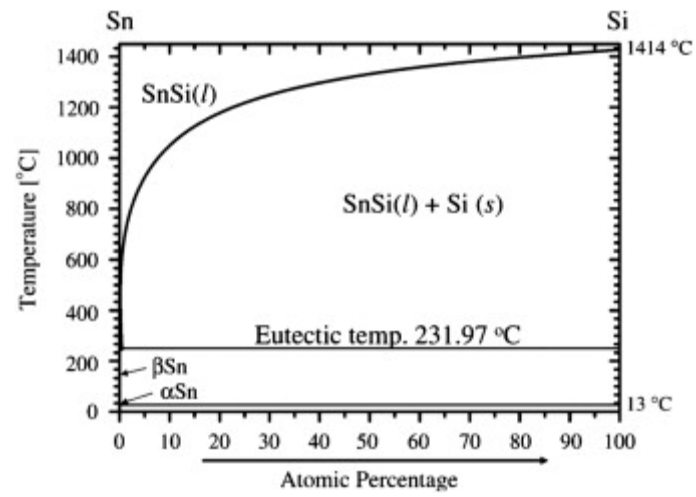


Fig. 7. Schematic of the surface tension and contact angle of the liquid/wire interface.

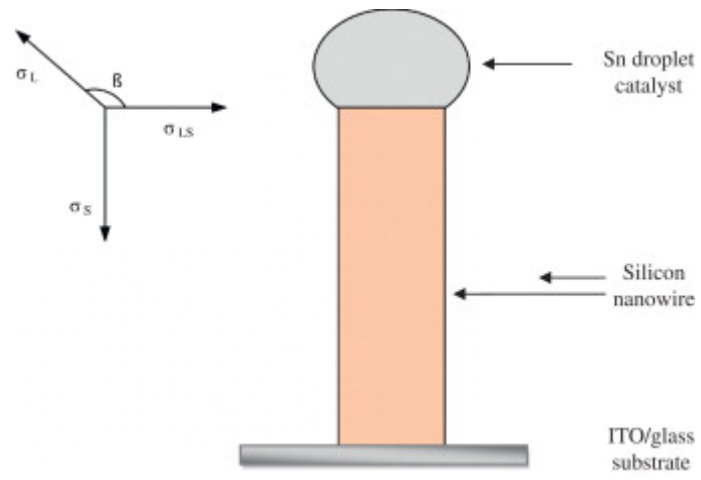


Fig. 8. XRD patterns of: (A) SiNWs prepared using Sn catalyst thin films with thickness 10–100 nm and (B) ITO-coated glass substrate.

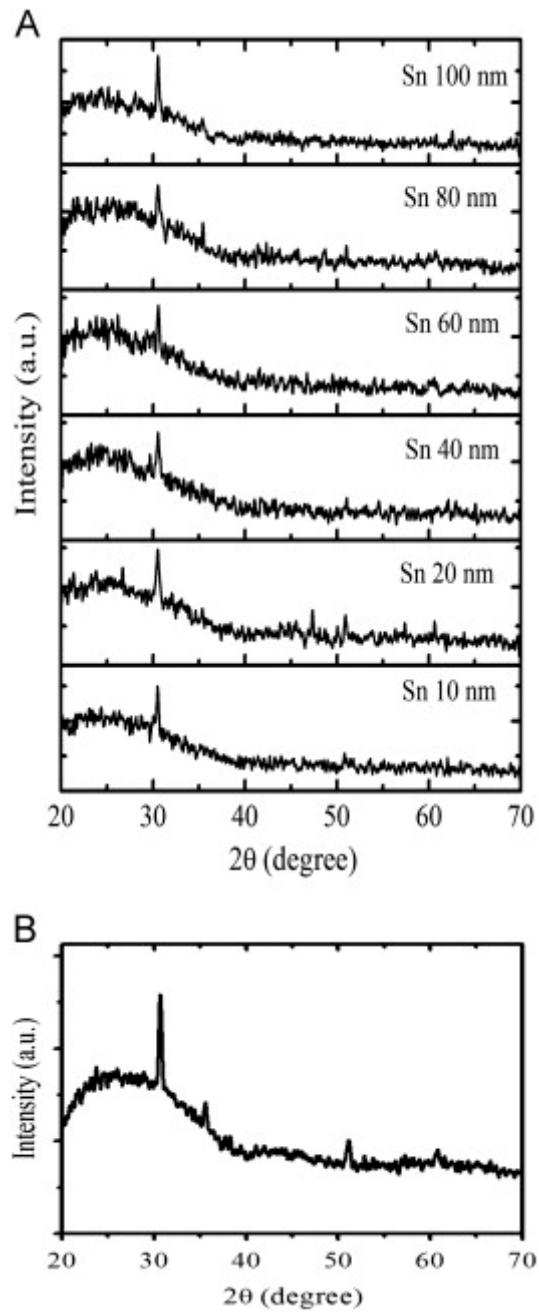


Table 1. Catalyst and nanowire diameters, liquid/wire interface tension, contact angle and wire density for SiNWs prepared with a Sn catalyst on ITO/glass.

Sn film thickness (nm)	Average catalyst diameter D_c (nm)	SiNWs diameter D_w (nm)	(R/r) Metal/wire contact angle β°	Surface tension σ_{LS} (J/m^2)	SiNWs density wire/ $(\mu m)^2$
10	96	75	1.28 129	0.37	17
20	105	96	1.1 115	0.25	15
40	120	105	1.14 119	0.29	13
60	138	136	1.02 101	0.11	11
80	201	185	1.09 113	0.23	8
100	211	194	1.08 112	0.22	8